



Cite this: DOI: 10.1039/d4na00133h

# Recent advances in the biosynthesis of ZnO nanoparticles using floral waste extract for water treatment, agriculture and biomedical engineering

Duyen Thi Cam Nguyen,<sup>a</sup> Ngoan Thi Thao Nguyen,<sup>ab</sup> Thuy Thi Thanh Nguyen<sup>b</sup>  
and Thuan Van Tran \*<sup>a</sup>

Flowers are often discarded after cultural and religious events, making it worthwhile to explore the utilization of this floral waste for material production. Floral extracts contain a diverse array of phytochemicals such as polyphenols, flavonoids, and reducing sugars, which play a significant role in the formation and influencing the properties of zinc oxide (ZnO) nanoparticles. In this review, we delve into the importance of floral extract, methodology, mechanism, and influencing factors in the production of ZnO nanoparticles. Additionally, the role of green ZnO nanoparticles as an adsorbent and photocatalyst for water treatment is discussed. These floral extract-mediated ZnO nanoparticles exhibit advantages in agricultural and biomedical applications, including promoting seed germination and demonstrating antibacterial, anticancer, and antifungal properties. Cost analysis reveals that while various expenses are associated with ZnO production, scaling up processes can help reduce these costs. This review underscores the potential of floral waste extract for the synthesis of green ZnO nanoparticles, thereby contributing to waste-to-wealth strategies and adhering to green chemistry principles.

Received 13th February 2024  
Accepted 29th May 2024

DOI: 10.1039/d4na00133h

rsc.li/nanoscale-advances

## 1. Introduction

Water stands as the most crucial resource essential for sustaining all life forms. The 2018 World Water Development Report, as issued by the United Nations, highlights a current annual global water demand escalation of 1%.<sup>1</sup> This trajectory indicates an impending scarcity of water resources. Persistent pollution compounds this challenge, with drinking water contamination, pharmaceutical residuals, heavy metals, and disruptions causing eutrophication in water bodies.<sup>2,3</sup> Alterations in the water cycle further exacerbate the issues, leading to adverse impacts on energy and agricultural production, human and animal health, as well as economic progress.<sup>4</sup> The level and duration of exposure to heavy metals significantly dictate the extent of toxic bioaccumulation in fish.<sup>5,6</sup> While some heavy metals serve as micronutrients essential for biological metabolism, they collectively induce harmful effects through metabolic interference and mutagenesis.<sup>7</sup> In the case of dyes, industrial dye wastewater results from various textile processing stages, often exceeding the quality benchmarks for wastewater treatment.<sup>8–10</sup> This wastewater contains colorants, waxes, and notably high pH levels, along with substantial chemical oxygen demand (COD).<sup>11</sup>

The mass discharge of flower waste into rivers significantly impacts the flora, fauna, and overall aquatic ecosystems.<sup>12</sup> This waste, originating from floral and religious sites; social events such as birthdays, weddings, and funerals; and recreational venues such as hotels and spas, raises significant concerns.<sup>13</sup> Every year, millions of tons of dried flowers from major religious sites globally find their way into rivers or become part of solid municipal waste.<sup>14</sup> Indeed, India alone produces approximately 4738 tons of floral waste daily, while Turkey generates around 50 tons of tulip petal waste annually.<sup>13</sup> Presently, there is a shortage of proper systems for segregating, collecting, transporting, and managing floral waste from religious sites and markets. As flowers enter water bodies, they elevate biological oxygen demand and worsen various wastewater indicators.<sup>12</sup> Moreover, the presence of pesticides in flowers leads to the introduction of unwanted pollutants into water bodies, significantly compromising the water quality.<sup>15</sup> Discarded flowers in open areas become breeding grounds for mosquitoes and other insects, thus emitting foul odors, polluting the land, and drastically diminishing the visual and aesthetic appeal of the surroundings.<sup>13</sup> The natural degradation of floral wastes also gives rise to environmental pollution by emitting methane and carbon dioxide.<sup>13</sup> Utilizing flower waste to extract valuable compounds for the synthesis of nanoparticles presents a viable approach, thereby simultaneously tackling environmental issues.

Nanomaterials with unique characteristics have become an integral part of cutting-edge research fields.<sup>16</sup> In the past years,

<sup>a</sup>Institute of Applied Technology and Sustainable Development, Nguyen Tat Thanh University, 298-300A Nguyen Tat Thanh, District 4, Ho Chi Minh City 755414, Vietnam. E-mail: tranuv@gmail.com; tramvt@ntt.edu.vn

<sup>b</sup>Nong Lam University - Ho Chi Minh City, Ho Chi Minh City 700000, Vietnam



ZnO nanoparticles have garnered enormous interest due to their versatile applications in solar cells, catalysts, antibacterial materials, gas sensors, luminescent materials, and photocatalysts.<sup>17–19</sup> Indeed, ZnO possesses n-type semiconducting properties, boasting a direct bandgap of nearly 3.2 eV.<sup>20</sup> Recent progress has shown that nano-ZnO can be used as a heterogeneous catalyst with low cost, non-toxicity, and environmental advantages.<sup>20–22</sup> On exposure to an irradiation source in wastewater, ZnO nanoparticles likely trigger the decomposition of organic pollutants.<sup>23</sup> This process generates free radicals such as  $\cdot\text{OH}$  and  $\cdot\text{O}_2^-$  that serve as potent oxidizing agents, facilitating photodegradation.<sup>24</sup> Additionally, semiconductor materials are used to functionalize ZnO, boosting its capacity to absorb visible light.<sup>25</sup> This enhancement significantly augments the efficiency of pollutant removal.

Although ZnO nanoparticles play a vital role in biomedical, catalysis, and electrochemical fields, many synthetic methods are toxic and often not eco-friendly.<sup>26–29</sup> Therefore, it is necessary to include an innovative approach for fabricating benign ZnO nanoparticles using floral waste extract resources.<sup>30</sup> A number of articles have indicated the content of phytochemicals such as flavonoids, alkaloids, phenolics, and tannins present in the flower parts of many plants.<sup>31–33</sup> These biocompounds supply a bio-capping and bio-stabilizing platform during the formation of nanoparticles.<sup>34</sup> These biogenically synthesized ZnO nanoparticles exhibit high performance comparative to chemically synthesized ones in several cases.<sup>35,36</sup> The proposition of synthesizing ZnO nanoparticles using flower waste extract can therefore be a feasible solution, extending applications in wastewater treatment.

Biological hazards, notably viruses, fungi, parasites, and bacteria, are major sources of infections and infectious diseases.<sup>37</sup> Green ZnO nanoparticles can show remarkable biomedical activity since the floral extract-based synthetic process results in these nanoparticles with biocompatible properties, making them readily applicable in biomedical fields.<sup>38</sup> For instance, green ZnO nanoparticles exhibit substantial toxicity against various multidrug-resistant microorganisms in humans.<sup>39</sup> While traditional cancer treatments like chemotherapy, radiotherapy, and surgery can have severe side effects on the human body, nanomedicine leveraging nanomaterials such as ZnO nanoparticles mitigate these side effects thanks to their high biocompatibility and cancer-targeting abilities.<sup>40</sup> The anticancer potential of ZnO nanoparticles is multifaceted, involving the induction of cancer cell apoptosis and autophagy.<sup>41</sup> Using ZnO nanoparticles biosynthesized using floral extract, these processes can be accelerated, facilitating the termination of cancer cells.

Previous reviews have extensively covered the synthesis and diverse applications of ZnO nanoparticles. For example, Alhujaily *et al.*<sup>42</sup> discussed the role of plant-based ZnO nanoparticles with emphasis on biomedical engineering fields including antimicrobial, antioxidant, anti-inflammatory, and tissue repair. Similarly, Rai *et al.*<sup>30</sup> showed recent advances in ZnO nanomaterials biosynthesized using different biological sources for targeted bioengineering applications. To the best of our knowledge, however, this study marks the first comprehensive discussion

regarding the utilization of flower waste extract to produce ZnO nanoparticles for both environmental and biomedical applications. This study systematically addresses innovative strategies in turning zero-cost floral waste into high value-added products including ZnO nanoparticles and ZnO-based composites. The effective utilization of floral waste for ZnO nanoparticles synthesis stands as a prime example of converting waste into valuable resources, pursuing a waste-to-wealth strategy, contributing to environmental protection and public health.

## 2. Green synthesis of ZnO nanoparticles using floral extract

### 2.1. Methodology for the synthesis of ZnO nanoparticles

There are a number of methods (biological, chemical, physical) for the synthesis of ZnO nanoparticles with emphasis on two different routes including top-down and bottom-up, as illustrated in Fig. 1. To be more specific, the top-down approach is a synthesis process that splits an original bulk material into ZnO particles with smaller sizes through ball milling, sputtering, laser ablation and thermal evaporation. Unfortunately, these mechanical and physical processes consume a large amount of energy and require well-equipped instruments; thus, they are not favorable in small production scale. Meanwhile, the bottom-up approaches such as hydrothermal, co-precipitation, chemical vapour deposition, and sol-gel cannot easily obtain a nano-scale size of ZnO particles but also requires a low energy source and simple equipment. However, the biggest disadvantage of this route is the use of toxic chemicals during the synthesis, causing adverse impacts on the environment and secondary pollution. To reach a critically safe and sustainable synthesis goal, the green synthesis of ZnO nanoparticles using green plant extract should be considered.

### 2.2. Sustainable aspects of green ZnO synthesis

Floral extract biomediated synthesis of ZnO nanoparticles holds several key advantages such as process without chemical use, safe production, low energy consumption, and favorability for laboratory scale (Fig. 2). It is known that flowers from plants can supply valuable bioactive compounds such as polyphenols, tannins, proteins, and alkaloids. These chemicals may take responsibility for the reduction and formation of ZnO nanoparticles. Instead of using toxic chemicals like alkaline and surfactant, natural phytochemicals extracted from flowers themselves act as reducing and capping agents in the production of ZnO nanoparticles. With the abundance of flower sources, the biosynthesis of ZnO nanoparticles should be nearly available. Therefore, the eco-friendly synthesis of ZnO nanoparticles using floral extract can meet the fundamental principles of green chemistry.

In plant species, their tissues such as leave, root, bark, and flower mostly contain natural phytochemicals, but flowers are very rich in antioxidants such as phenolics, tannins, and reducing sugars. For example, a recent study determined the chemical composition of *Pogostemon cablin* Linn. flower and leaf by GC-MS analysis.<sup>31</sup> The authors found that patchouli alcohol (27.5%) and caryophyllene (18.2%) were major





Fig. 1 Top-down and bottom-up routes for the production of ZnO nanoparticles.



Fig. 2 Several advantages of green synthesis of ZnO using floral extract.

constituents in flower. *Mimusops elengi* flower was found to have above 70 different compounds including flavonoids, alkaloids, phenolics, and tannins.<sup>32</sup> In another example, a recent study compared the chemical composition of *Pogostemon cablin* Linn. flower and leaf by HPLC-MS and GC-MS analyses.<sup>33</sup> The authors found phenylpropanoids (>30%) and a series of phytochemicals and their derivatives such as tannins, flavonoids, alkaloids, benzene, and phenylpropanoids. However, the flower extract possessed 189 compounds, compared with 174 compounds in the leaves extract and 87 compounds in green coffee beans extract. As expected, the flower extract exhibited the highest ABTS radical scavenging activity among the samples. Therefore, the natural compounds from the flower extract can be a potential for the biosynthesis of ZnO nanoparticles.

### 2.3. Formation of green ZnO nanoparticles

The formation mechanism of ZnO nanoparticles is complicated and worth considering. It is acknowledged that the floral

extracts are very rich in main natural compounds such as polyphenol, tannin, saponin, and alkaloid, and many of them are strong antioxidants. In the presence of Zn(II) ions, these phytochemical compounds act as reducing and capping agents. As described, the change in the color from light blue to white after 180 min of reaction indicates the formation of Zn<sup>2+</sup>-diisobutyl phthalate complex (Fig. 3). It is presumable that the  $\pi$  electrons of the oxygenated groups are donated to the empty d-orbitals of Zn<sup>2+</sup> through coordination bonds. Thanks to the complexation and chelation between phytochemicals and Zn(II) ions, ZnO nanoparticles are less aggregated, well dispersed, and highly stable. Moreover, ZnO nanoparticles synthesized using floral extract often exhibit a higher degree of surface chemistry in comparison to those synthesized using chemical methods.

*Jacaranda mimosifolia* flower extract has been used in the biosynthesis of ZnO nanoparticles.<sup>44</sup> The researchers determined the presence of oleic acid in the flower extract *via* gas chromatography-mass spectrometry analysis, and this natural compounds acted as a capping agent. The complexation between Zn<sup>2+</sup> and oleic acid could be due to the electrostatic interaction between them, allowing the formation of well-dispersed ZnO under microwave irradiation heating for 5 min (Fig. 4). To elucidate the surface chemistry of green ZnO nanoparticles, a recent research group compared the ZnO synthesis between the chemical method using NaBH<sub>4</sub> as a reducing agent and the biogenic method using flower extract from *Nerium oleander*.<sup>45</sup> They indicated that the shift of the FTIR absorption peak of the Zn–O bond might be as a result of the biofunctional groups from *Nerium oleander* flower extract. The surface of biogenic ZnO nanoparticles was found to be rich in functional groups such as hydroxyl, carbonyl and amine, indicating the role of floral extract in the production of ZnO. The same observation was reported for the biosynthesis of ZnO nanoparticles using *Moringa oleifera* extract, with L-ascorbic





Fig. 3 (a) Visual image of *Anchusa italica* flowers, the color change of *Anchusa italica* flower extract before (b) and after (c) the addition of  $Zn^{2+}$  ions after 360 min, (d) a proposed mechanism of the complexation interaction between diisobutyl phthalate from *Anchusa italica* floral extract and  $Zn^{2+}$  ions and the formation of biogenic ZnO nanoparticles after calcination. Reproduced with permission of Elsevier from ref. <sup>43</sup>. Copyright 2016.

acid converting into L-dehydroascorbic acid to form free radicals and interact with  $Zn(II)$ .<sup>46</sup>

#### 2.4. Effect of factors on the green synthesis of ZnO nanoparticles

According to Table 1, the shape of biogenic ZnO nanoparticles synthesized using floral extract is very diverse, including spherical (%), rod (%), semi-spherical, hexagonal, cubic, and semicircular (%) (Fig. 5). A majority of spherical shape of green ZnO nanoparticles could be because the complexation between  $Zn^{2+}$  and phytochemicals hinders the aggregation of particles during the nucleation and crystal growth. Therefore, their spherical shape can be maintained. The particle size of green ZnO nanoparticles is in the range from 8 nm to 90 nm (Table 1). The distribution of particle size seems to be equivalent to the ZnO particle size synthesized using plant extract, algae, bacterial and fungi.<sup>47</sup>

Because of the difference in the chemical composition of each floral extract, many factors such as floral extract concentration, pH of the solution, and calcination temperature are likely to affect the morphology, shape, particle size, etc., of biogenic ZnO nanoparticles. The particle sizes of ZnO are often found to show a downward decrease with an increase in the concentration of the floral extract.<sup>34</sup> This can be due to the fact that the presence of more natural bioactive compounds as capping agents enhances the complexation between  $Zn^{2+}$  and

them. As a result, ZnO nanoparticles synthesized using floral extract often exhibit a lower degree of aggregation and particle size in comparison to those synthesized using chemical methods.

Moreover, the addition of floral extract into  $Zn^{2+}$  solution can increase the interaction between  $Zn^{2+}$  and phytochemicals, but an excess of floral extract can lead to the breaking of the complex stability. For example, *Nyctanthes arbor-tristis* flower extract volume from 0.25 mL to 2 mL was tested to check the intensity of the prominent peak at 346 nm.<sup>59</sup> The authors found that a volume at 1 mL of the flower extract per 50 mL of 0.01 M  $Zn^{2+}$  solution obtained the maximum absorption intensity (Fig. 6). The same trend in the pH factor was observed since the authors changed the pH from 9 to 13. The intensity of the peak tended to increase with the increase in the pH and showed a maximum absorption (362 nm) at pH 12.

## 3. Applications of ZnO nanoparticles biosynthesized using floral extract

### 3.1. Adsorption

Adsorption is commonly a preferable method to treat polluted wastewaters. This method acquires some advantages such as high performance, simplicity, ease of operation, and eco-friendly property. Considering green ZnO nanoparticles as an adsorbent, the adsorption of pollutants can occur by some





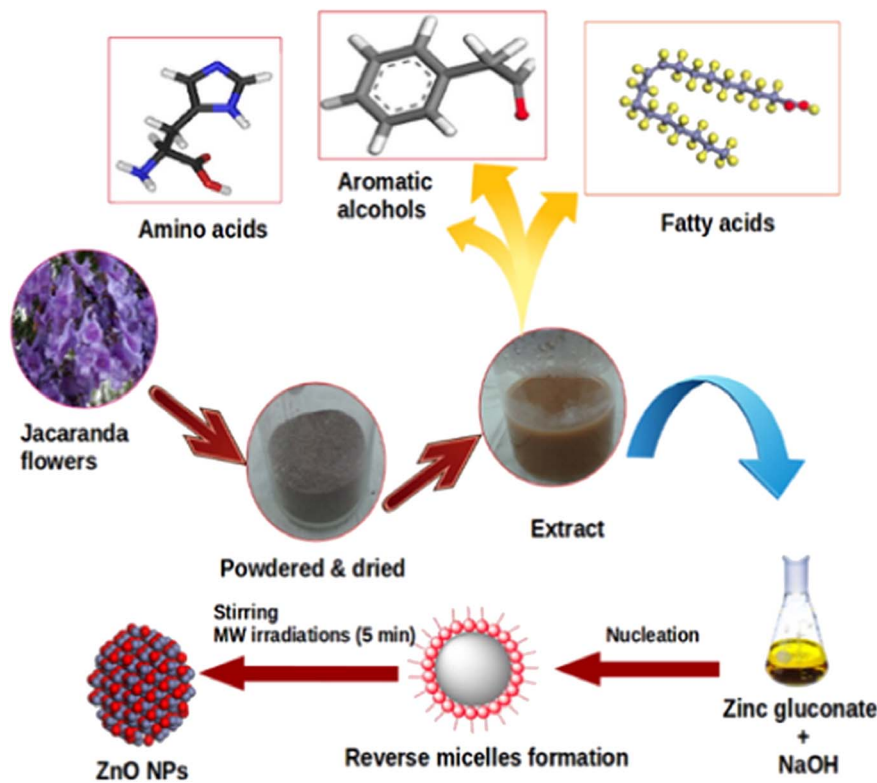


Fig. 4 The biosynthesis of ZnO nanoparticles with the aid of oleic acid inherent in *Jacaranda mimosifolia* flower extract. Reproduced with permission of Elsevier from ref. <sup>44</sup>. Copyright 2016.

possible mechanisms such as electrostatic interaction. Moreover, the incorporation of floral extract can supply some functional groups, e.g., phenolic and carboxyl groups on the surface of ZnO nanoparticles, facilitating the adsorption process.

Some studies synthesized green ZnO nanoparticles using floral extract for the removal of pollutants in water. For example, Nguyen *et al.* successfully biosynthesized ZnO nanoparticles using *Canna indica* L. flowers extract with an average particle size of 27.8 nm.<sup>49</sup> To be more specific, the authors designed an optimization model based on minimum-run resolution IV with a multivariate model to remove Coomassie brilliant blue G-250 in water. It was found that 70.8% of this dye was eliminated by a chemisorbed monolayer adsorption. Several possible interactions between Coomassie brilliant blue G-250 dye and ZnO nanoparticles biosynthesized using *Canna indica* L. flowers extract was suggested with emphasis on electrostatic type, hydrogen bonding, Yoshida hydrogen bonding, and  $n-\pi$  type (Fig. 7).

In another work, *Bougainvillea spectabilis* flowers were used to create the extract for the synthesis of ZnO.<sup>48</sup> In this study, green ZnO nanoparticles could enhance the removal of 2,4-dinitrophenol at an equilibrium capacity of 42.6–70.4 mg g<sup>-1</sup>. The authors demonstrated that the removal of 2,4-dinitrophenol by green ZnO nanoparticles was endothermic with an enthalpy ( $\Delta H$ ) value of 7.38 kJ mol<sup>-1</sup>. However, the uptake capacity obtained in this work was still relatively low, and the removal efficiency was not very high. Considering the effectiveness of green ZnO nanoparticles, a combined photocatalytic

and sonocatalytic process should be applied for the better removal efficiency of 2,4-dinitrophenol contaminant.

### 3.2. Catalytic degradation

Green ZnO nanoparticles-based photocatalysts can participate in the degradation of organic pollutants, typically organic textile dyes such as methylene blue, Congo red, and crystal violet in water. Normally, these ZnO nanoparticles catalyze the photocatalytic reaction under ultraviolet or visible light irradiation. Indeed, the biosynthesis of ZnO nanoparticles was reported with the use of *Hibiscus sabdariffa* flower extract for dye degradation.<sup>50</sup> The results revealed that 97% of methylene blue dye could be degraded in 150 min in the presence of ZnO catalysts and an ultraviolet irradiation source. The photocatalytic performance of ZnO was explained due to the uptake of the dye on the catalyst surface through  $\pi-\pi$  interactions between benzene rings derived from the floral extract. However, a very high ratio of floral extract (8%) did not promote the catalytic activity of ZnO, which might be due to light blockage by the surface coverage of the floral extract.

*Lantana camara* flower extract was also used for the biosynthesis of ZnO nanoparticles.<sup>51</sup> In this study, the authors applied a photocatalytic system based on UV light/ZnO to degrade methylene blue dye. A photodegradation efficiency of 98% was obtained after 75 min under an optimum pH of 10. The researchers explained that the migration of OH<sup>-</sup> ions into the surface of the catalyst could lead to the generation of 'OH



Table 1 Synthesis and application of green ZnO nanoparticles synthesized using floral extract

Plant names	Shape	Particle size (nm)	Bandgap (eV)	Applications	Main findings	Ref.
<i>Bougainvillea spectabilis</i>	Hexagonal	12–31	—	Wastewater treatment	Removal of 2,4-dinitrophenol, 42.6–70.4 mg g <sup>-1</sup> by adsorption; photocatalytic route was 84.4%, and by sonocatalysis was 77.1%	48
<i>Canna indica</i>	Spherical	27.8	3.08	Wastewater treatment, seed germination	Removal of Coomassie brilliant blue G-250 by adsorption (31.1 mg g <sup>-1</sup> ), photocatalytic degradation (94.2%), promoting seed germination	49
<i>Hibiscus sabdariffa</i>	Semicircular	8.7–38.6	2.77–2.96	Wastewater treatment	Photocatalytic degradation of methylene blue dye at 97%	50
<i>Lantana camara</i>	Spherical	21.4–27.2	3.56	Wastewater treatment	Degradation of methylene blue 98% under UV light	51
<i>Chrysanthemum</i> spp.	Spherical	9.1–17.9	1.92–1.98	Wastewater treatment	Degradation of Congo red 95% under UV light	52
<i>Trifolium pratense</i>	Spherical	60–70	—	Antibacterial	Zones of growth inhibition at 100 µg mL <sup>-1</sup> against <i>S. aureus</i> (22–31 mm), <i>E. coli</i> (22–31 mm), <i>P. aeruginosa</i> (21–28 mm), <i>S. aureus</i> (24–31 mm), <i>P. aeruginosa</i> (14–29 mm)	53
<i>Jacaranda mimosifolia</i>	Spherical	8–11	4.03	Antibacterial	Cell viability at 100 µg mL <sup>-1</sup> in <i>E. coli</i> (48%) and <i>E. faecium</i> (43%)	44
<i>Matricaria chamomilla</i>	Cubic	41.0	—	Antibacterial	Cell viability against strain GZ 0003 of <i>Xanthomonas oryzae</i> of 79.4%	54
<i>Punica granatum</i>	Spherical	53	—	Antibacterial	Minimum inhibitory concentration against <i>B. cereus</i> and <i>M. catarrhalis</i> of 0.61 µg mL <sup>-1</sup>	55
<i>Clitoria ternatea</i>	Rod	84	—	Antibacterial	Zones of growth inhibition at 100 µg mL <sup>-1</sup> against <i>E. coli</i> (21.2 mm) and <i>S. aureus</i> (17 mm)	56
<i>Peltophorum pterocarpum</i>	Spherical	69.45	—	Antibacterial	Zones of growth inhibition at 100 µg mL <sup>-1</sup> against <i>B. cereus</i> (9–12 mm) and <i>E. coli</i> (9–10 mm)	57
<i>Clitoria ternatea</i>	Rod	84	—	Anticancer	IC <sub>50</sub> of 12.1 µg mL <sup>-1</sup> against breast cancer cells	56
<i>Hibiscus sabdariffa</i>	Spherical, semi-spherical	50.7 (ZnO)	—	Anticancer	Inhibitory concentration IC <sub>50</sub> against breast cancer cells of 33.5 µg mL <sup>-1</sup>	58
<i>Hibiscus sabdariffa</i>	Spherical, semi-spherical	51.6 (Au/ZnO)	—	Anticancer	Inhibitory concentration IC <sub>50</sub> against breast cancer cells of 34.9 µg mL <sup>-1</sup>	58
<i>Peltophorum pterocarpum</i>	Spherical	69.45	—	Anticancer	Cell viability at 10 µg mL <sup>-1</sup> against HeLa cancer cell lines of <i>Xanthomonas oryzae</i> of 50%	57
<i>Nyctanthes arbor-tristis</i>	Spherical	12–32	—	Antifungal	Minimum inhibitory concentration at 256 µg mL <sup>-1</sup> against <i>A. alternate</i> (64 µg mL <sup>-1</sup> ), <i>A. niger</i> (16 µg mL <sup>-1</sup> ), <i>B. cinerea</i> (128 µg mL <sup>-1</sup> ), <i>F. oxysporum</i> (64 µg mL <sup>-1</sup> ) and <i>P. expansum</i> (128 µg mL <sup>-1</sup> )	59

radicals to engage in the degradation of methylene blue dye. More interestingly, the green ZnO catalyst was very stable since a recyclability study was performed up to five times. Almost 80% of the degradation efficiency was retained during the final cycle, suggesting the role of the floral extract in increasing the stability of the ZnO catalyst.

Although the ZnO nanoparticles can efficiently catalyze the degradation of toxic dyes, the introduction of ultraviolet irradiation in the reaction was not preferred. Nguyen *et al.* used ZnO biosynthesized using *Canna indica* flowers extract as a catalyst for the removal of methylene blue dye (94.2%) in the presence of solar light.<sup>49</sup> In this work, a scavenging study was



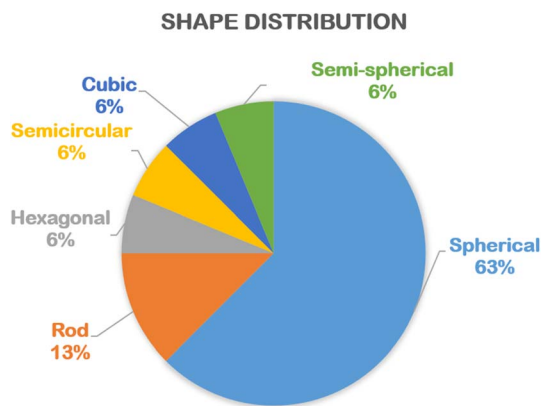


Fig. 5 The percentage of various shapes of biogenic ZnO nanoparticles synthesized using floral extract. Statistical data was collected from the relevant references cited in this work.

conducted, which confirmed the major role of  $\cdot\text{O}_2^-$  radicals in the photocatalytic degradation reaction. The importance of radicals followed the order  $\cdot\text{OH} < \text{h}^+ < \cdot\text{O}_2^-$ . Taking advantage of solar irradiation as a photogenerated source may make the ZnO-catalyzed degradation reaction more beneficial in the real application.

At the same trend, *Chrysanthemum* spp. floral waste was extracted and used to synthesize  $\text{ZnFe}_2\text{O}_4/\text{ZnO}$

nanocomposites.<sup>52</sup> Accordingly, an incorporation amount of  $\text{ZnFe}_2\text{O}_4$  was investigated at 0–50%. As a fuel, the flower extract supplied several functional groups such as hydroxyl and carbonyl for enriching the surface of the nanocomposite (Fig. 8). This allows to create more interactions between Congo red dye and the catalyst, enhancing the adsorption on the surface of  $\text{ZnFe}_2\text{O}_4/\text{ZnO}$ . The authors carried out the photocatalytic degradation of Congo red using  $\text{ZnFe}_2\text{O}_4$ -50%/ZnO in the presence of solar light irradiation. They found that the best photocatalytic activity was at nearly 95%, compared with 44% of bare ZnO. Moreover, this catalyst could be recovered easily by inducing a simple magnet. The pathways of Congo red degradation in the presence of the ZnO-based catalyst can be more elucidated, as illustrated in Fig. 9. With more than 3 cycles of reusability, the green nanoparticles were expected to be a promising catalyst for the degradation of toxic dyes.

### 3.3. Seed germination

Seed germination is a physiological process in plants under a favorable environment condition during their life stage.<sup>60</sup> The tests of seed germination enable to understand how plants deal with environmental change as well as determine whether they can persist.<sup>61</sup> The interaction between plants and polluted soil or water is on the basis of evaluating the quality of treated water.

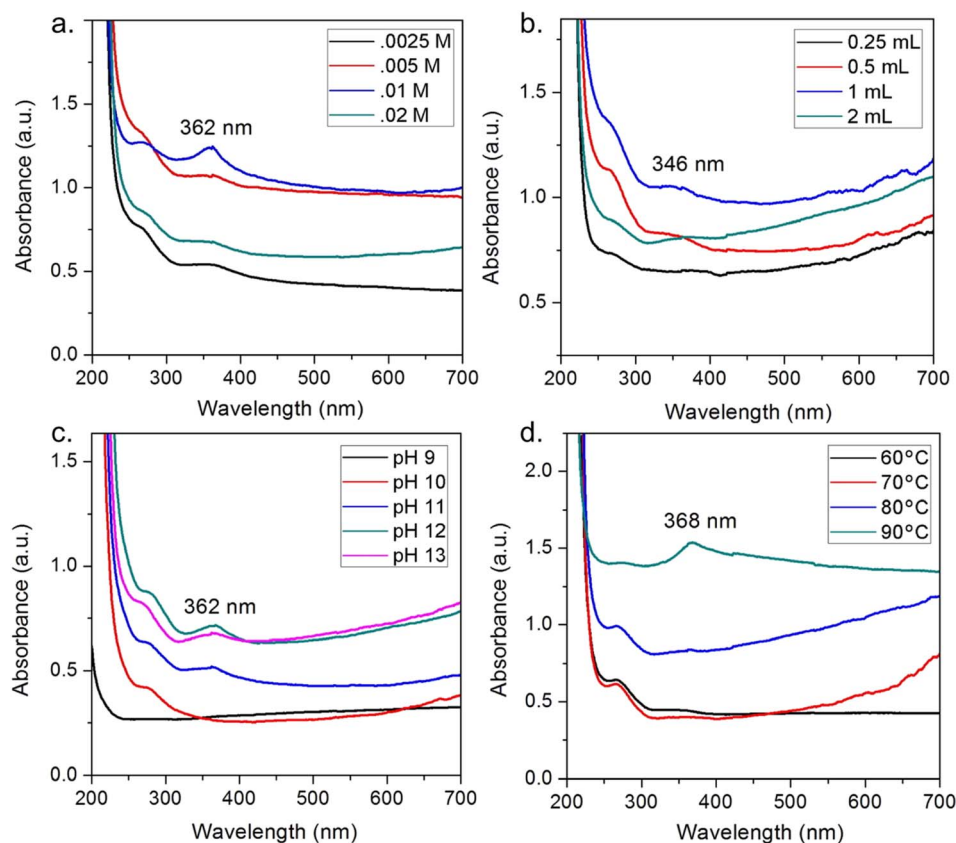


Fig. 6 Effect of factors on ZnO biosynthesis using *Nyctanthes arbor-tristis* floral extract, (a) concentration of  $\text{Zn}^{2+}$ , (b) volume of floral extract added into 50 mL of 0.01 M  $\text{Zn}^{2+}$  solution, (c) pH of the solution, (d) temperature of the solution. Reproduced with permission of Elsevier from ref. <sup>59</sup>. Copyright 2018.



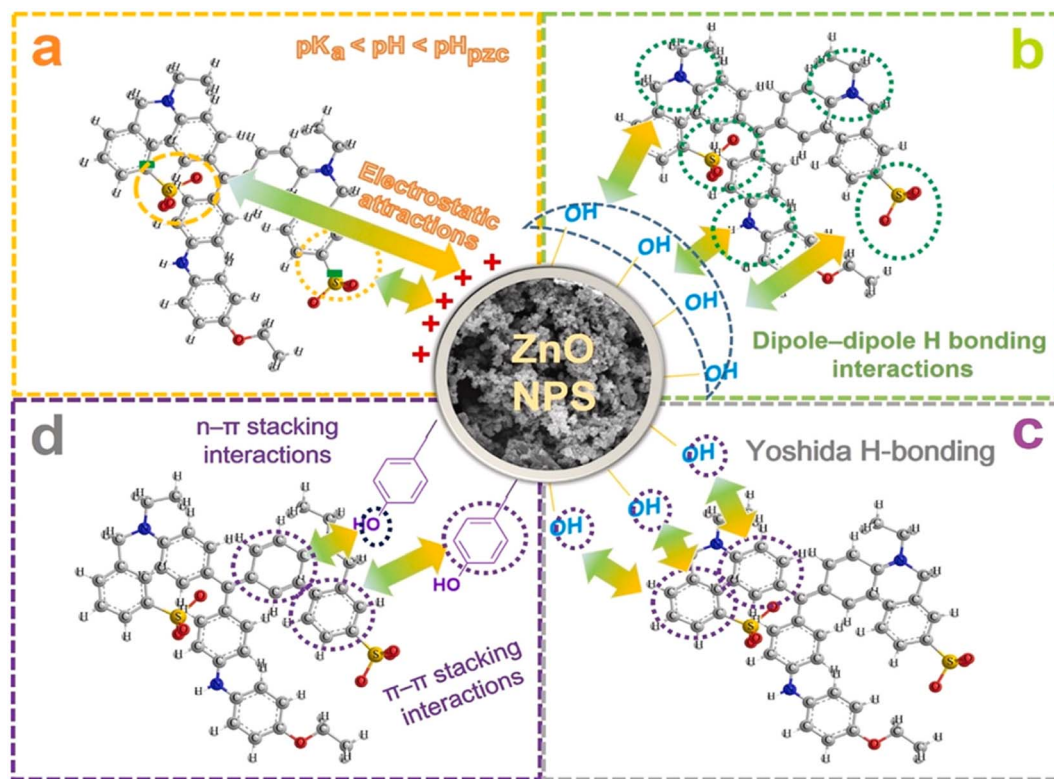


Fig. 7 Proposed interactions between Coomassie brilliant blue G-250 dye and ZnO nanoparticles biosynthesized using *Canna indica* L. flowers extract. Reproduced with permission of Elsevier from ref. <sup>49</sup>. Copyright 2021.

To check the safety of the toxic dye-contaminated water treated by *Canna indica* L. flower extract-mediated ZnO nanoparticles, Nguyen *et al.* carried out a seed germination experiment with emphasis on the green and red bean seedlings.<sup>49</sup> After five days of treatment, the beans grew normally compared with the control samples (Fig. 10). More interestingly, the root and shoot of bean cultivated in ZnO-treated water samples seemed to develop better. The authors suggested that the release of  $Zn^{2+}$  with a very tiny amount avoided root rot since  $Zn^{2+}$  acted as an antibacterial agent. Moreover,  $Zn^{2+}$  could be a micronutrient during the seed germination of bean. In other words, bean seedling might adsorb the  $Zn^{2+}$  released from ZnO nanoparticles as an essential micronutrient element for their growth and development.

In another study,  $ZnFe_2O_4$ -ZnO nanocomposites biosynthesized using *Chrysanthemum* spp. floral waste obtained the same excellent seed germination of bean samples.<sup>52</sup> The researchers observed that the average body length (14.7 cm) of bean seedlings grown in treated dye wastewater reached a higher value than that (13.3 cm) of the sample grown in water. However, the underlying mechanisms of antibacterial process and root development were still not elucidated. Seed germination test and mechanism by green ZnO nanoparticles should therefore be more investigated.

### 3.4. Antibacterial activity

Multi-drug resistance as a result of using antibiotic improperly has led to tremendous difficult in the treatment of bacterial

infection.<sup>62</sup> The application of biomediated nanoparticles in biomedical treatment may be a feasible strategy due to their biocompatibility and high activity.<sup>63</sup> A number of studies showed excellent antibacterial activity of floral extract-based green ZnO nanoparticles against biohazard pathogenic strains including Gram-negative and Gram-positive bacteria, as listed in Table 1.

For example, green ZnO nanoparticles biosynthesized from *Jacaranda mimosifolia* flower extract have been used as antibacterial agents.<sup>44</sup> The authors applied gas chromatography-mass spectrometry (GC-MS) analysis to confirm the presence of oleic acid in the flower extract, which acted as a capping agent. Moreover, the facet-specific binding of this compound on the surface of ZnO nanoparticles was simulated on the basis of interaction energy using a computational chemistry tool. Spherical ZnO nanoparticles in this study resulted in a cell viability against *E. coli* (48%) and *E. faecium* (43%), better than those (51–59%) under the chemically synthesized ZnO nanoparticles. Green ZnO nanoparticles have higher biocompatibility, easily penetrating the outer membrane into the intracellular environment, causing a damage to the cell components. In another study, *Trifolium pratense* flower extract with main natural compounds such as anthocyanin, phenolic acid, and tannin was used to synthesize ZnO nanoparticles.<sup>53</sup> Accordingly, green ZnO nanoparticles offered an outstanding antibacterial performance, *i.e.*, zones of growth inhibition against *S. aureus* (22–31 mm), *E. coli* (22–31 mm), *P. aeruginosa* (21–28 mm), *S. aureus* (24–31 mm), and *P. aeruginosa* (14–29





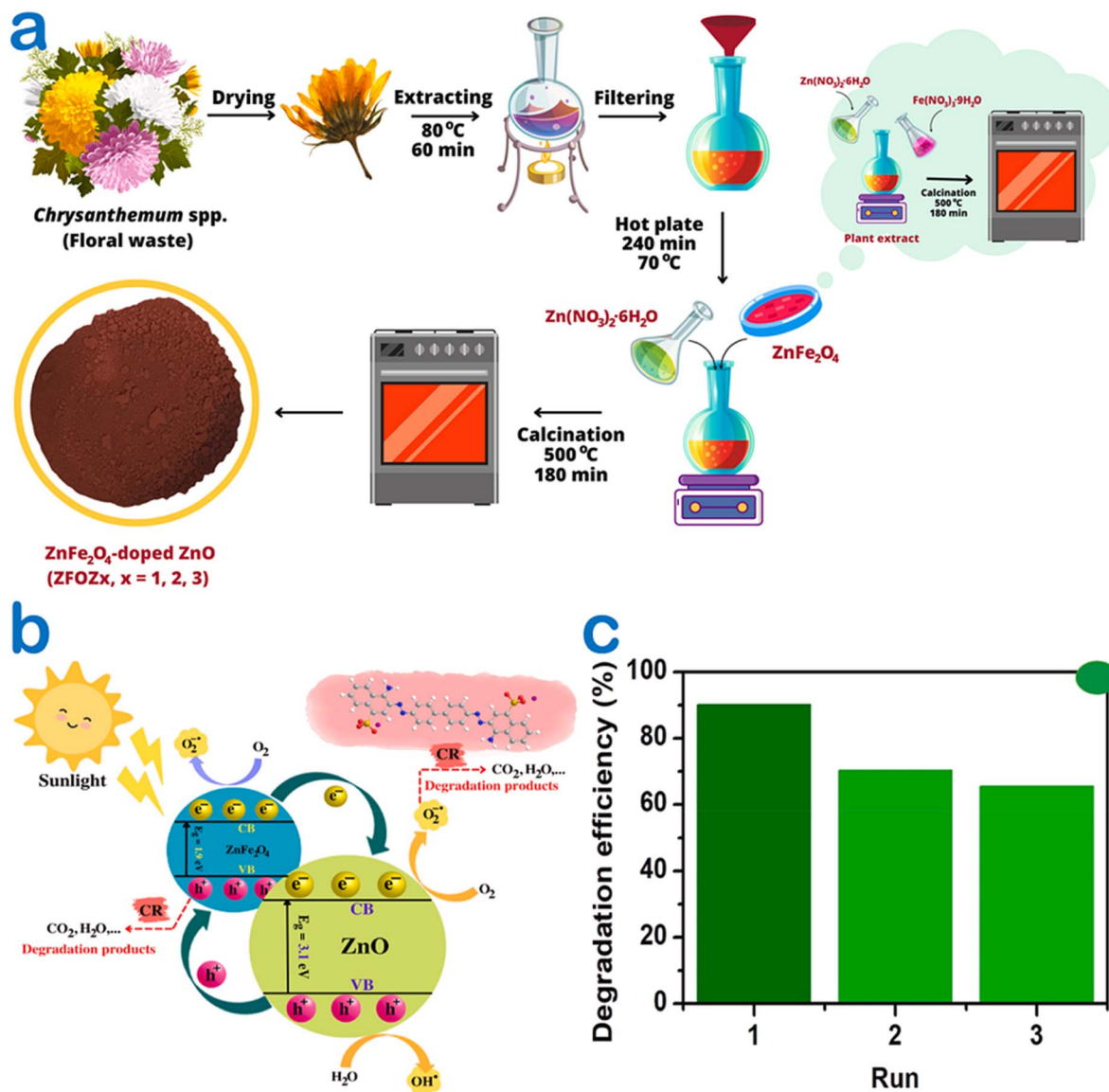


Fig. 8 (a) A schematic illustration of ZnFe<sub>2</sub>O<sub>4</sub>/ZnO nanocomposites biosynthesized using the *Chrysanthemum* spp. floral waste extract, (b) several plausible photocatalytic mechanisms under green ZnFe<sub>2</sub>O<sub>4</sub>-50%/ZnO catalysis for the degradation of the Congo red dye, (c) a recyclable run of ZnFe<sub>2</sub>O<sub>4</sub>-50%/ZnO for the degradation of the Congo red dye in the presence of solar light irradiation. Reproduced with permission of Elsevier from ref. <sup>52</sup>. Copyright 2023.

mm). It can be explained that ZnO nanoparticles released Zn<sup>2+</sup> into cell membranes, attacked bacterial cells by causing the extrusion of the cytoplasmic contents and caused cell death.

To compare the antibacterial performance of ZnO nanoparticles synthesized using various green sources, Ogunyemi *et al.* used three kinds of extracts from chamomile (*Matricaria chamomilla*) flower, olive leaf, and red tomato fruit.<sup>54</sup> Xoo strain GZ 0003, as a bacterial target of *Xanthomonas oryzae*, was tested and is illustrated in Fig. 11. The results showed that ZnO synthesized from olive leaf extract gave the highest zone of growth inhibition (22 mm) at 16.0 μg mL<sup>-1</sup>, which was higher than that (17 mm) of chamomile floral extract-based ZnO nanoparticles. The antibacterial activity difference among ZnO nanoparticles could be possibly due to the effect of natural

compounds in the extract. The researchers found that olive leaves contained many phytochemicals such as terpenes, flavonoids, saponins, and tannins, which acted as reducing and capping agents. As a result, the average particle size of ZnO biosynthesized using this extract obtained the smallest value (41 nm) compared with 51.2–51.6 nm for the others. It was known that smaller particles of ZnO can lead to an easier entry into the bacterial membrane to terminate the cell.<sup>26</sup> The antibacterial mechanism of the ZnO nanoparticles was attributable to the formation of reactive oxygen species including HO<sub>2</sub><sup>·</sup>, O<sub>2</sub><sup>-</sup>, and <sup>·</sup>OH. They react with proteins and lipids of the membrane, leaking the key components such as cytoplasm, causing damage to DNA and RNA in the cell and leading to cell death.



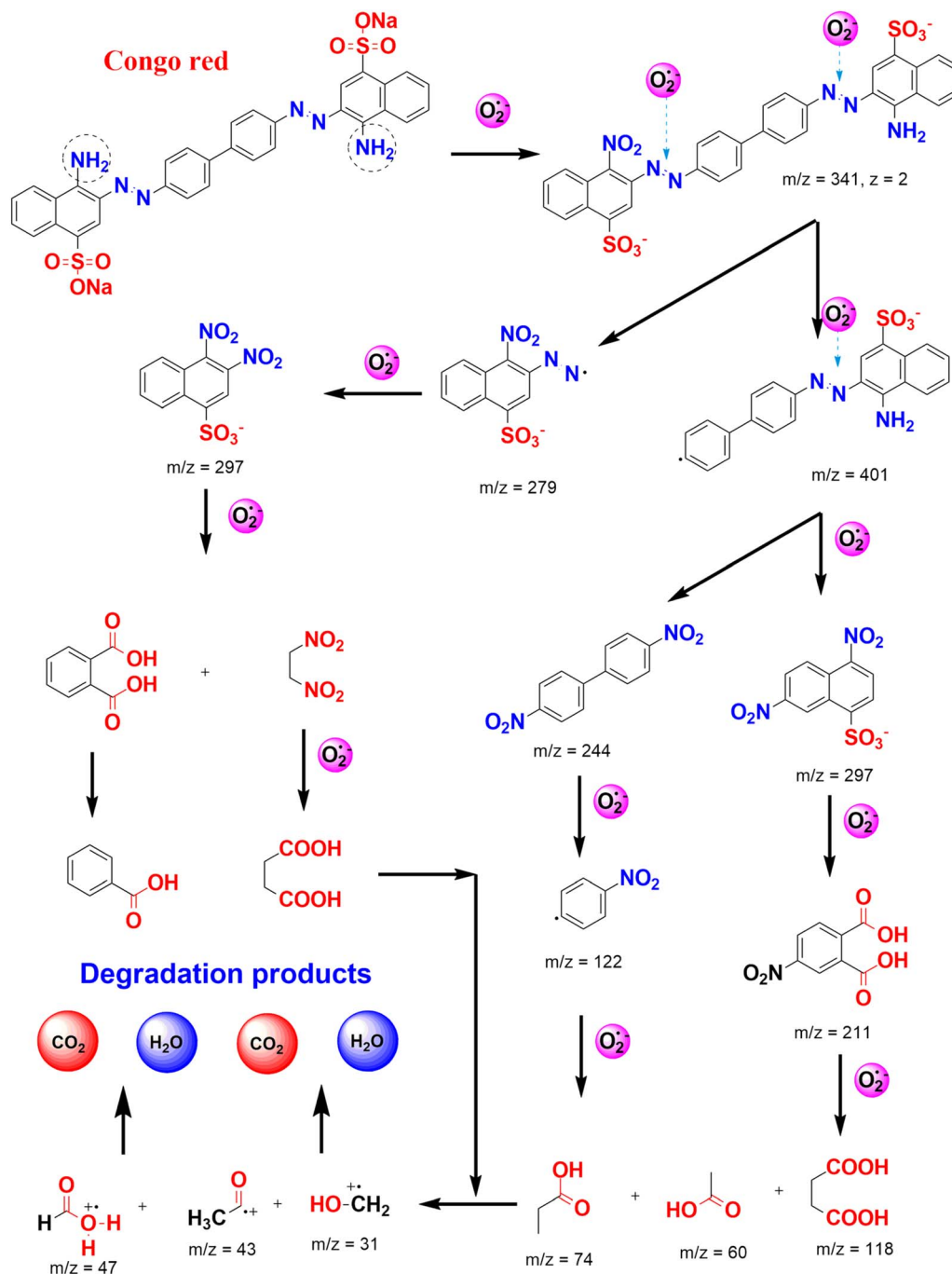


Fig. 9 Several plausible pathways for Congo red degradation in the presence of reactive oxygen species photo-generated under the ZnO-based catalyst.

Towards another comparison, *Punica granatum* leaves and flower extract were used to produce ZnO nanoparticles.<sup>55</sup> The results showed that smaller minimum inhibitory concentrations against a wide range of bacterial species such as *S. aureus*, *B. cereus*, *P. aeruginosa*, *K. pneumoniae*, *S. typhi*, *E. faecalis*, and *E. faecium* of ZnO bio-produced using floral extract were observed, indicating higher antibacterial activity. A recent study also reported promising ZnO synthesis using *Senna auriculata* extract against both Gram-positive and Gram-negative bacteria.<sup>64</sup> It can

therefore be suggested that floral extract-mediated ZnO nanoparticles can be one of the effective and eco-friendly bacterial agents.

### 3.5. Anticancer activity

Cancer, caused by an unbridled growth of cancerous cells, damages and impacts adjacent normal cells and is acknowledged as one of the most lethal and intricate diseases.<sup>65</sup> Although a number of various treatments including surgery,



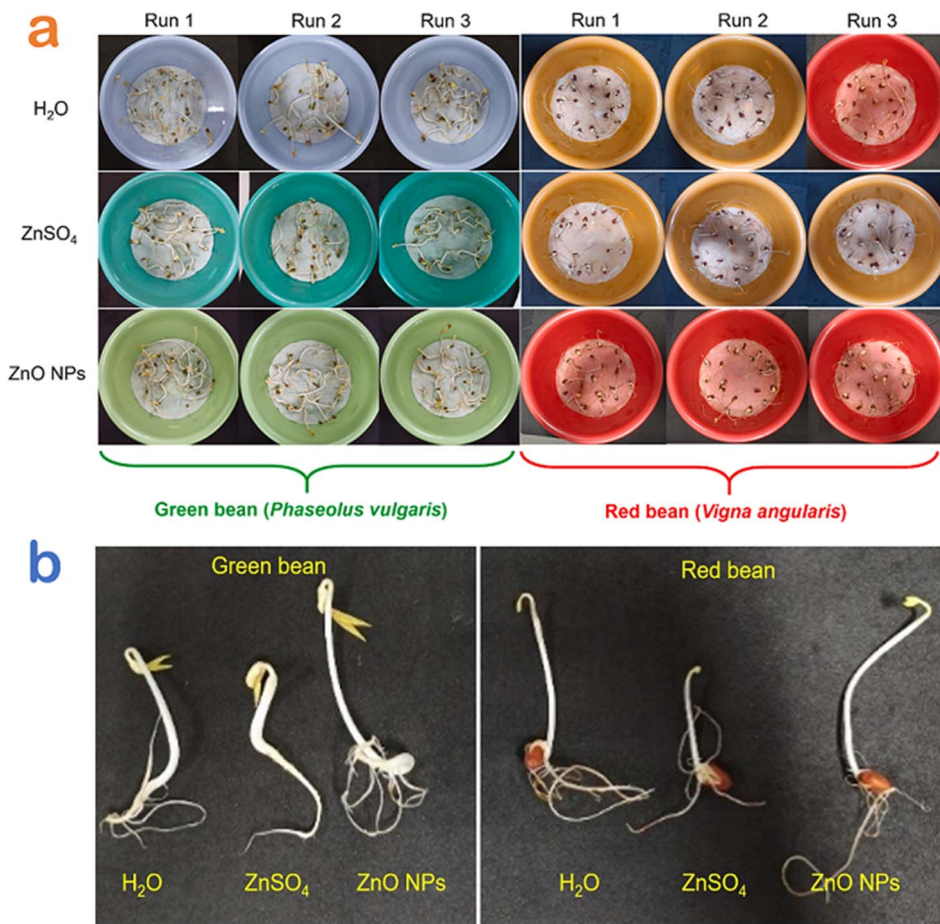


Fig. 10 (a) Seed germination experiments and (b) several seedling samples for the green and red bean seedling in Congo red wastewater samples treated by H<sub>2</sub>O, ZnSO<sub>4</sub> and ZnO nanoparticles using *Canna indica* L. flower extract. Reproduced with permission of Elsevier from ref. <sup>49</sup>. Copyright 2021.

radiation therapy, and chemotherapy have been developed for cancer treatment, these interventions have potential risk towards human health.<sup>66</sup> Over the past years, the green floral extract-mediated nanoparticles have been applied as a promising alternative against cancer diseases (Table 1).

Very recently, Shochah and Jabir produced green ZnO nanoparticles using *Hibiscus sabdariffa* flower extract as a natural bioreducing and biocapping agent.<sup>58</sup> The authors observed that the half-maximal inhibitory concentration of green ZnO against breast cancer cells was 33.5  $\mu\text{g mL}^{-1}$ . However, the result of the anticancer activity obtained in this study was relatively low. To address this drawback, a modification step of ZnO nanoparticles was considered (Fig. 12). The authors developed a composite by decorating Au onto ZnO nanoparticles using the same extract, giving an inhibitory concentration of 34.9  $\mu\text{g mL}^{-1}$ . Unfortunately, the anticancer performance of the composite in comparison with Au-undoped ZnO was not improved since green Au/ZnO had a lower cytotoxicity against the cancer cell lines.

Alahmdi *et al.* tested the anticancer performance of ZnO nanoparticles synthesized from the extract of *Clitoria ternatea* flower.<sup>56</sup> In this study, green ZnO nanoparticles exhibited

a strong cytotoxicity against breast cancer cells with a half-maximal inhibitory concentration (IC<sub>50</sub>) value of 12.1  $\mu\text{g mL}^{-1}$ . This result was so far better than the study reported by Shochah and coworkers.<sup>58</sup> For the mechanism of ZnO nanoparticles, the authors explained that intracellular reactive oxygen species and caspase-3 activation by ZnO nanoparticles caused apoptosis alterations such as chromatin condensation and nucleus disintegration, leading to DNA injury and death in breast cancer cells.

### 3.6. Antifungal activity

Fungal phytopathogens adversely affect the growth and development of plants, reducing the crop productivity of industrial plants, causing a spreading epidemic and a threat to global food security.<sup>67</sup> Nanoparticles can be used as an antifungal agent against fungal pathogens.<sup>34</sup> Green ZnO nanoparticles exhibited an excellent antifungal activity according to a past study.<sup>59</sup> Accordingly, *Nyctanthes arbor-tristis* flowers were extracted and used for the biosynthesis of ZnO nanoparticles. The report showed that this bionanoparticle could inhibit all phytopathogens including *A. alternate* (64  $\mu\text{g mL}^{-1}$ ), *A. niger* (16  $\mu\text{g mL}^{-1}$ ), *B. cinerea* (128  $\mu\text{g mL}^{-1}$ ), *F. oxysporum* (64  $\mu\text{g mL}^{-1}$ ) and *P.*





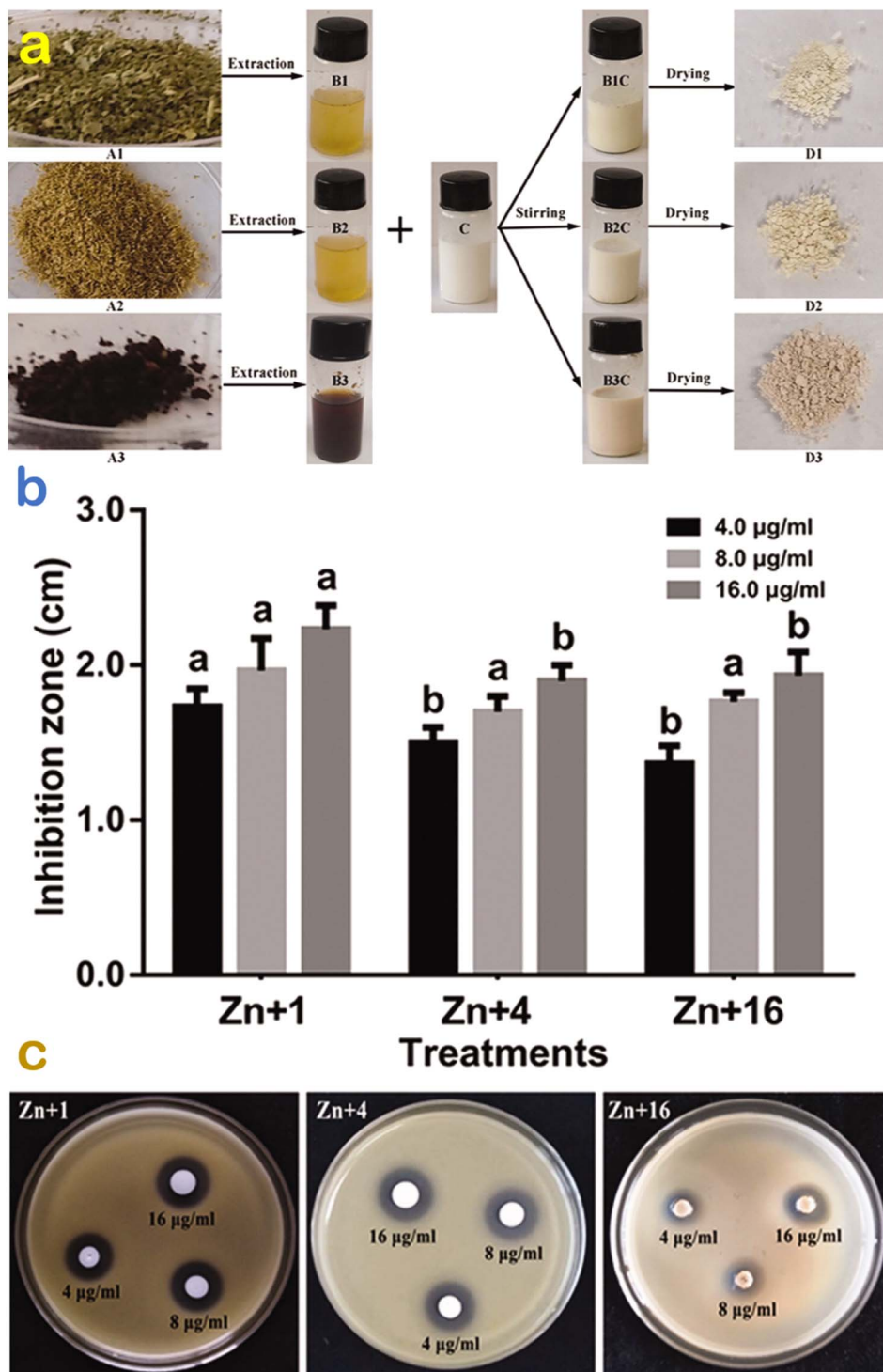


Fig. 11 (a) Green synthesis of ZnO nanoparticles synthesis using *Olea europaea*, *Matricaria chamomilla* flower, and *Lycopersicon esculentum* extracts; (b) their respective antibacterial performance; and (c) their respective inhibition zones against strain GZ 0003 against *Xanthomonas oryzae*. Reproduced with permission from Taylor & Francis from ref. <sup>54</sup>. Copyright 2019.

*expansum* ( $128 \mu\text{g mL}^{-1}$ ). The authors explained a possible mechanism against fungal phytopathogens based on the contact and disruption of the cell membrane. It was suggested that  $\text{H}_2\text{O}_2$  may generate reactive oxygen species such as  $\text{O}_2^{\cdot-}$ ,  $\cdot\text{OH}$ , and  $\text{HO}_2^{\cdot}$ , which terminated the key physiological processes of fungal cell, resulting in cell death.

#### 4. Cost analysis

For synthesis of adsorbent materials, the cost estimation is required before the commercialization and large-scale production. Cost estimation of green ZnO production is likely dependent on many factors including





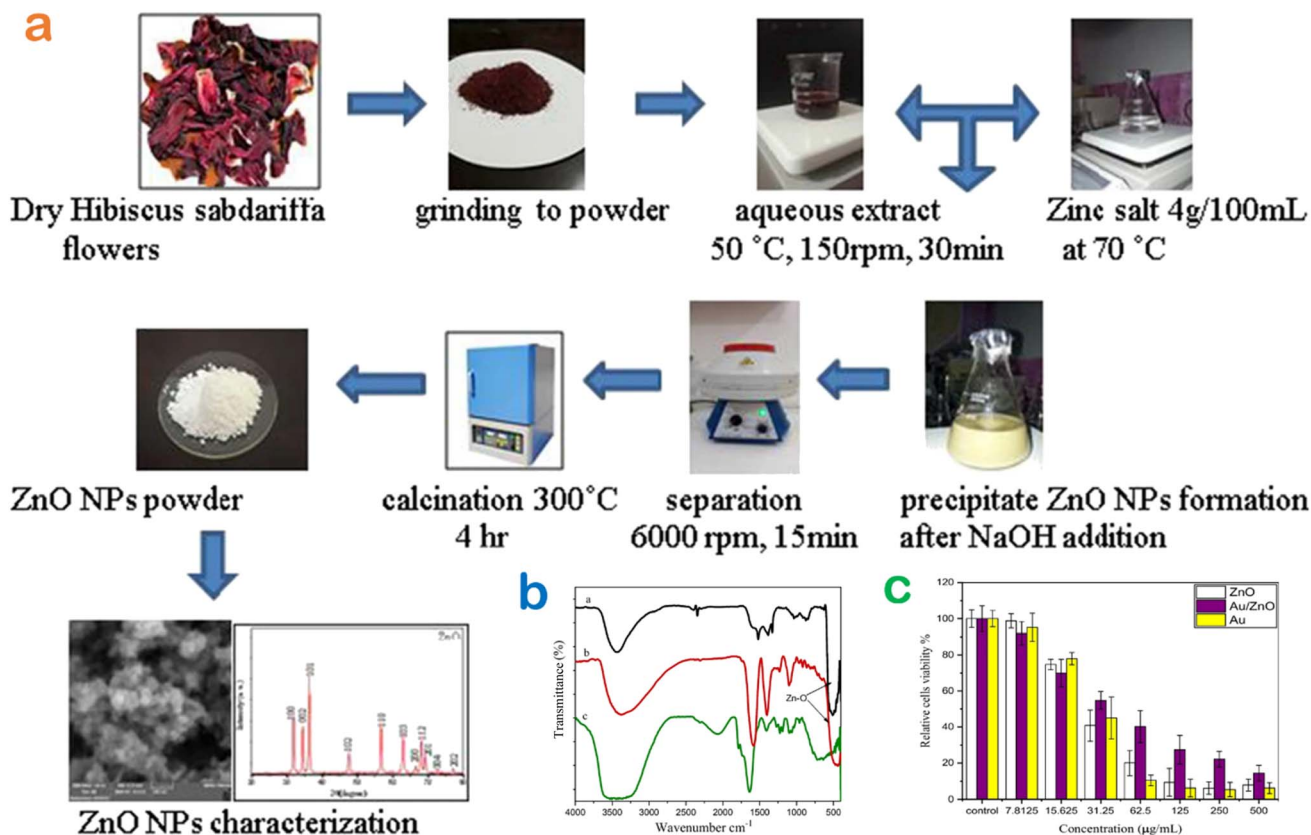


Fig. 12 (a) A biosynthesis route of ZnO nanoparticles using *Hibiscus sabdariffa* flower extract; (b) surface chemistry of bio-based nanomaterials ZnO and Au/ZnO compared with the extract; (c) MTT assay to evaluate the toxicity of green ZnO, Au, Au/ZnO nanoparticles against MCF-7 cell lines. Reproduced with permission of Springer Nature from ref. <sup>58</sup>. Copyright 2023.

(i) Cost of floral waste collection and pretreatment. However, floral waste is free of charge or zero-cost.

(ii) Cost of compulsory chemicals (zinc salts) and other chemicals (H<sub>2</sub>O, ethanol, etc.) or extraction of floral waste.

(iii) Cost of transportation.

(iv) Cost of chemical modification (optional for the production of ZnO-based composites).

(v) Labor expenditure.

(vi) Cost of storage/preservation.

(vii) Cost of electricity.

(viii) Cost of equipment and technical maintenance.

Although many costs are included, three kinds of costs can be main contributors, including chemicals, labor expenditure, and equipment. For chemicals, ZnCl<sub>2</sub> cost is estimated at about US\$14 per kg, while deionized H<sub>2</sub>O cost for extraction is so far lower, at about US\$0.1 per liter. For labor expenditure, this cost varies depending on countries, e.g., US\$3.0 per hour or US\$30 per ten hours for Vietnam's labor cost (Statista, 2020). Similarly, experimental equipment cost is dependent on many factors, can be estimated based on the market price of ZnO nanoparticles. Generally, the total production cost of green ZnO nanoparticles synthesized using floral waste extract can range from US\$60 to US\$100 per kg. It should be noted that the scaling process can reduce this cost.

## 5. Conclusions

The present work underlined the importance, mechanism, factors, and potential of floral extract for the green synthesis of ZnO nanoparticles. The utilization of floral extract brings the main advantages of safety, simplicity, and effectiveness. Phytochemicals present in floral extract contribute significantly to the formation and properties of green ZnO nanoparticles. For adsorption application, floral extract-mediated ZnO nanoparticles act as a promising adsorbent to remove organic pollutants including dyes and 2,4-dinitrophenol. These ZnO nanoparticles efficiently catalyze the photocatalytic reaction to degrade methylene blue, Congo red, etc., under ultraviolet or visible light irradiation. Incorporating dopants such as ZnFe<sub>2</sub>O<sub>4</sub> enhance the photocatalytic activity of the ZnO-based nanocomposites. Green ZnO nanoparticles show the advantages of seed germination and antimicrobial activity. Although the production of floral extract-mediated ZnO nanoparticles can include many kinds of cost, these costs can be reduced through the scaling-up processes. This work suggests an innovative approach of using floral waste extract to biosynthesize ZnO, reaching a waste-to-wealth strategy and obtaining highly valuable products.



## Ethical statement

The authors declare that the manuscript has not been published anywhere nor submitted to another journal. The manuscript is not currently being considered for publication in any other journal. All authors have been personally and actively involved in substantive work leading to the manuscript, and will hold themselves jointly and individually responsible for its content. Research does not involve any human participants and/or animals.

## Code availability

The authors declare that software application or custom code supports their published claims and comply with field standards.

## Data availability

The authors declare that all data and materials support their published claims and comply with field standards.

## Author contributions

Duyen Thi Cam Nguyen contributed to conceptualization, investigation, methodology, writing – original draft. Ngoan Thi Thao Nguyen contributed to validation, data curation, writing – review & editing. Thuy Thi Thanh Nguyen contributed to formal analysis, data curation, writing – review & editing. Thuan Van Tran contributed to conceptualization, writing – original draft, writing – review & editing, supervision, project administration. All authors read and approved the final manuscript.

## Conflicts of interest

The authors declare that there are no conflicts of interest.

## Acknowledgements

This research is funded by Foundation for Science and Technology Development Nguyen Tat Thanh University, Vietnam.

## References

- 1 X. Gu, Z. Li, K. Gao, P. Mei, Z. Zhang and W. Jiang, *Highlights in Science, Engineering and Technology*, 2023, **33**, 227–235.
- 2 I. Karaouzas, N. Kapetanaki, A. Mentzafou, T. D. Kanellopoulos and N. Skoulidakis, *Chemosphere*, 2021, **263**, 128192.
- 3 A. Yadav, E. R. Rene, M. Sharma, V. Kumar, M. K. Mandal and K. K. Dubey, *Curr. Pollut. Rep.*, 2023, **9**, 391–409.
- 4 P. D'Odorico, J. Carr, C. Dalin, J. Dell'Angelo, M. Konar, F. Laio, L. Ridolfi, L. Rosa, S. Suweis, S. Tamea and M. Tuninetti, *Environ. Res. Lett.*, 2019, **14**, 053001.
- 5 A. S. Shafuiddin Ahmed, S. Sultana, A. Habib, H. Ullah, N. Musa, M. Belal Hossain, M. Mahfujur Rahman and M. Shafiqul Islam Sarker, *PLoS One*, 2019, **14**, e0219336.
- 6 O. A. Ajala, M. R. Oke, T. F. Ajibade, F. O. Ajibade, B. Adelodun, J. O. Ighalo, M. O. Ajala, P. Kumar, H. Demissie, A. Y. Uguya, I. D. Sulaymon and L. F. O. Silva, *Environ. Sci. Pollut. Res.*, 2022, **29**, 82660–82680.
- 7 N. H. Ghorji, T. Ghorji, M. Q. Hayat, S. R. Imadi, A. Gul, V. Altay and M. Ozturk, *Int. J. Environ. Sci. Technol.*, 2019, **16**, 1807–1828.
- 8 T. Islam, M. R. Repon, T. Islam, Z. Sarwar and M. M. Rahman, *Environ. Sci. Pollut. Res.*, 2023, **30**, 9207–9242.
- 9 P. O. Oladoye, M. O. Bamigboye, O. D. Ogunbiyi and M. T. Akano, *Groundw. Sustain. Dev.*, 2022, **19**, 100844.
- 10 M. Shabir, M. Yasin, M. Hussain, I. Shafiq, P. Akhter, A.-S. Nizami, B.-H. Jeon and Y.-K. Park, *J. Ind. Eng. Chem.*, 2022, **112**, 1–19.
- 11 N. R. J. Hynes, J. S. Kumar, H. Kamyab, J. A. J. Sujana, O. A. Al-Khashman, Y. Kuslu, A. Ene and B. Suresh Kumar, *J. Cleaner Prod.*, 2020, **272**, 122636.
- 12 S. Dey, G. Taraka Naga Veerendra, S. S. Anjaneya Babu Padavala and A. V. Phani Manoj, *Water-Energy Nexus*, 2023, **6**, 187–230.
- 13 S. Dutta and M. S. Kumar, *J. Cleaner Prod.*, 2021, **294**, 126280.
- 14 V. Kumar, S. Kumari and P. Kumar, in *Environmental Degradation: Causes and Remediation Strategies*, Agro Environ Media – Agriculture and Environmental Science Academy, Haridwar, India, 2020, pp. 154–165.
- 15 N. Akhtar, M. I. Syakir Ishak, S. A. Bhawani and K. Umar, *Water*, 2021, **13**, 2660.
- 16 A. Hajjafari, S. Sadr, A. Rahdar, M. Bayat, N. Lotfalizadeh, S. Dianaty, A. Rezaei, S. P. Moghaddam, K. Hajjafari, P. A. Simab, Z. Kharaba, H. Borji and S. Pandey, *Inorg. Chem. Commun.*, 2024, **164**, 112409.
- 17 V. Vinitha, M. Preeyanghaa, V. Vinesh, R. Dhanalakshmi, B. Neppolian and V. Sivamurugan, *Emergent Mater.*, 2021, **4**, 1093–1124.
- 18 Z. Jiang, B. Liu, L. Yu, Y. Tong, M. Yan, R. Zhang, W. Han, Y. Hao, L. Shangguan, S. Zhang and W. Li, *J. Alloys Compd.*, 2023, **956**, 170316.
- 19 M. Saeed, H. M. Marwani, U. Shahzad, A. M. Asiri and M. M. Rahman, *Chem. Rec.*, 2024, **24**, e202300106.
- 20 F. M. Sanakousar, C. Vidyasagar, V. M. Jiménez-Pérez and K. Prakash, *Mater. Sci. Semicond. Process.*, 2022, **140**, 106390.
- 21 N. Bhattacharjee, I. Som, R. Saha and S. Mondal, *Int. J. Environ. Anal. Chem.*, 2022, 1–28.
- 22 P. Dhull, A. Sudhaik, P. Raizada, S. Thakur, V.-H. Nguyen, Q. Van Le, N. Kumar, A. A. Parwaz Khan, H. M. Marwani, R. Selvasembian and P. Singh, *Chemosphere*, 2023, **333**, 138873.
- 23 S. Kim, N. Son, S.-M. Park, C.-T. Lee, S. Pandey and M. Kang, *Catalysts*, 2023, **13**, 567.
- 24 K. A. Sultana, M. T. Islam, J. A. Silva, R. S. Turley, J. A. Hernandez-Viezas, J. L. Gardea-Torresdey and J. C. Noveron, *J. Mol. Liq.*, 2020, **307**, 112931.
- 25 A. Annam Renita, S. Sathish, P. S. Kumar, D. Prabu, N. Manikandan, A. Mohamed Iqbal, G. Rajesh and G. Rangasamy, *J. Environ. Manage.*, 2023, **344**, 118614.



- 26 N. T. T. Nguyen, L. M. Nguyen, T. T. T. Nguyen, T. T. Nguyen, D. T. C. Nguyen and T. V. Tran, *Environ. Chem. Lett.*, 2022, **20**, 2531–2571.
- 27 O. A. Zelekew, H. H. Haitosa, X. Chen and Y.-N. Wu, *Adv. Colloid Interface Sci.*, 2023, **317**, 102931.
- 28 P. Dhiman, G. Rana, A. Kumar, G. Sharma, D. V. N. Vo and M. Naushad, *Environ. Chem. Lett.*, 2022, **20**, 1047–1081.
- 29 A. Kavitha, A. Doss, R. P. Praveen Pole, T. P. K. Pushpa Rani, R. Prasad and S. Satheesh, *Biocatal. Agric. Biotechnol.*, 2023, **48**, 102654.
- 30 R. S. Rai, G. J. P, V. Bajpai, M. I. Khan, N. Elboughdiri, A. Shanableh and R. Luque, *Environ. Res.*, 2023, **221**, 114807.
- 31 S. K. Pandey, R. Gogoi, S. Bhandari, N. Sarma, T. Begum, S. Munda, M. Lal and J. Essent, Oil Bear, *Plants*, 2022, **25**, 160–179.
- 32 P. K. Rout, D. Sahoo and L. N. Misra, *Ind. Crops Prod.*, 2010, **32**, 678–680.
- 33 X. Shen, F. Nie, H. Fang, K. Liu, Z. Li, X. Li, Y. Chen, R. Chen, T. Zheng and J. Fan, *Food Sci. Nutr.*, 2023, **11**, 917–929.
- 34 N. T. T. Nguyen, L. M. Nguyen, T. T. T. Nguyen, R. K. Liew, D. T. C. Nguyen and T. V. Tran, *Sci. Total Environ.*, 2022, **827**, 154160.
- 35 S. Faisal, H. Jan, S. A. Shah, S. Shah, A. Khan, M. T. Akbar, M. Rizwan, F. Jan, U. Wajid, N. Akhtar, A. Khattak and S. Syed, *ACS Omega*, 2021, **6**, 9709–9722.
- 36 S. Mahalakshmi, N. Hema and P. P. Vijaya, *BioNanoScience*, 2020, **10**, 112–121.
- 37 R. E. Baker, A. S. Mahmud, I. F. Miller, M. Rajeev, F. Rasambainarivo, B. L. Rice, S. Takahashi, A. J. Tatem, C. E. Wagner, L. F. Wang, A. Wesolowski and C. J. E. Metcalf, *Nat. Rev. Microbiol.*, 2022, **20**, 193–205.
- 38 V. Devra, in *Agri-Waste and Microbes for Production of Sustainable Nanomaterials*, Elsevier, 2021, pp. 47–77.
- 39 S. M. F. Gad El-Rab, A. E. Abo-Amer and A. M. Asiri, *Curr. Microbiol.*, 2020, **77**, 1767–1779.
- 40 Y. Q. Liu, X. L. Wang, D. H. He and Y. X. Cheng, *Phytomedicine*, 2021, **80**, 153402.
- 41 S. B. Ghaffari, M. H. Sarrafzadeh, M. Salami and M. R. Khorramzadeh, *Int. J. Biol. Macromol.*, 2020, **151**, 428–440.
- 42 M. Alhujaily, S. Albukhaty, M. Yusuf, M. K. A. Mohammed, G. M. Sulaiman, H. Al-Karagoly, A. A. Alyamani, J. Albaqami and F. A. AlMalki, *Bioengineering*, 2022, **9**, 541.
- 43 S. Azizi, R. Mohamad, A. Bahadoran, S. Bayat, R. A. Rahim, A. Ariff and W. Z. Saad, *J. Photochem. Photobiol., B*, 2016, **161**, 441–449.
- 44 D. Sharma, M. I. Sabela, S. Kanchi, P. S. Mdluli, G. Singh, T. A. Stenström and K. Bisetty, *J. Photochem. Photobiol., B*, 2016, **162**, 199–207.
- 45 M. Khalil and F. Z. Alqahtany, *J. Inorg. Organomet. Polym. Mater.*, 2020, **30**, 3750–3760.
- 46 N. Matinise, X. G. G. Fuku, K. Kaviyarasu, N. Mayedwa and M. Maaza, *Appl. Surf. Sci.*, 2017, **406**, 339–347.
- 47 M. Bandeira, M. Giovanela, M. Roesch-Ely, D. M. Devine and J. da Silva Crespo, *Sustainable Chem. Pharm.*, 2020, **15**, 100223.
- 48 M. Nouri-Mashiran, L. Taghavi, E. Fataei, G. Ebrahimzadeh-Rajaei and M. Ramezani, *Main Group Chem.*, 2022, **21**, 559–575.
- 49 D. T. C. Nguyen, H. T. N. Le, T. T. Nguyen, T. T. T. Nguyen, L. G. Bach, T. D. Nguyen and T. V. Tran, *J. Hazard. Mater.*, 2021, **420**, 126586.
- 50 C. A. Soto-Robles, P. A. Luque, C. M. Gómez-Gutiérrez, O. Nava, A. R. Vilchis-Nestor, E. Lugo-Medina, R. Ranjithkumar and A. Castro-Beltrán, *Results Phys.*, 2019, **15**, 102807.
- 51 M. Swamy M, S. BS, M. C, P. S and R. ND, *Environ. Nanotechnol., Monit. Manage.*, 2021, **15**, 100442.
- 52 N. T. T. Nguyen, L. M. Nguyen, T. T. T. Nguyen, N. H. Nguyen, D. H. Nguyen, D. T. C. Nguyen and T. V. Tran, *J. Environ. Manage.*, 2023, **326**, 116746.
- 53 R. Dobrucka and J. Długaszewska, *Saudi J. Biol. Sci.*, 2016, **23**, 517–523.
- 54 S. O. Ogunyemi, Y. Abdallah, M. Zhang, H. Fouad, X. Hong, E. Ibrahim, M. M. I. Masum, A. Hossain, J. Mo and B. Li, *Artif. Cells, Nanomed., Biotechnol.*, 2019, **47**, 341–352.
- 55 U. L. Ifeanyichukwu, O. E. Fayemi and C. N. Ateba, *Molecules*, 2020, **25**, 4521.
- 56 M. I. Alahmdi, S. Khasim, S. Vanaraj, C. Panneerselvam, M. A. A. Mahmoud, S. Mukhtar, M. A. Alsharif, N. S. Zidan, N. E. Abo-Dya and O. F. Aldosari, *J. Inorg. Organomet. Polym. Mater.*, 2022, **32**, 2146–2159.
- 57 G. Khara, H. Padalia, P. Moteriya and S. Chanda, *Arabian J. Sci. Eng.*, 2018, **43**, 3393–3401.
- 58 Q. R. Shochah and F. A. Jabir, *Biomass Convers. Biorefin.*, 2023, 1–14.
- 59 P. Jamdagni, P. Khatri and J. S. Rana, *J. King Saud Univ., Sci.*, 2018, **30**, 168–175.
- 60 P. Poschlod, M. Abedi, M. Bartelheimer, J. Drobnik, S. Rosbakh and A. Saatkamp, *Veg. Ecol.*, 2nd edn, 2013, pp. 164–202.
- 61 E. Fernández-Pascual, A. Carta, A. Mondoni, L. A. Cavieres, S. Rosbakh, S. Venn, A. Satyanti, L. Guja, V. F. Briceño, F. Vandellook, E. Mattana, A. Saatkamp, H. Bu, K. Sommerville, P. Poschlod, K. Liu, A. Nicotra and B. Jiménez-Alfaro, *New Phytol.*, 2021, **229**, 3573–3586.
- 62 V. Singh and K. Chibale, *Acc. Chem. Res.*, 2021, **54**, 2361–2376.
- 63 N. T. T. Nguyen, L. M. Nguyen, T. T. T. Nguyen, U. P. N. Tran, D. T. C. Nguyen and T. V. Tran, *Chemosphere*, 2023, **312**, 137301.
- 64 S. Chandrasekaran, V. Anbazhagan and S. Anusuya, *Appl. Biochem. Biotechnol.*, 2023, **195**, 3840–3854.
- 65 Z. Yu, L. Gao, K. Chen, W. Zhang, Q. Zhang, Q. Li and K. Hu, *Nanoscale Res. Lett.*, 2021, **16**, 88.
- 66 H. Ranji-Burachaloo, P. A. Gurr, D. E. Dunstan and G. G. Qiao, *ACS Nano*, 2018, **12**, 11819–11837.
- 67 S. V. Avery, I. Singleton, N. Magan and G. H. Goldman, *Fungal Biol.*, 2019, **123**, 555–557.

